Distributed Model Predictive Control for Active Power Regulation in AC Microgrids

Xiao, Junjie; Wang, Lu; Bauer, Pavol; Qin, Zian

DOI
10.1109/IPEMC-ECCEAsia60879.2024.10567413

Publication date
2024

Document Version
Final published version

Published in
2024 IEEE 10th International Power Electronics and Motion Control Conference, IPEMC 2024 ECCE Asia

2024 IEEE 10th International Power Electronics and Motion Control Conference (IPEMC2024-ECCE Asia) | 979-8-3503-5133-0/24/$31.00 ©2024 IEEE | DOI: 10.1109/IPEMC-ECCEAsia60879.2024.10567413

Distributed Model Predictive Control for Active Power Regulation in AC Microgrids

Junjie Xiao
Electrical Sustainable Energy
Delft University of Technology
Delft, The Netherlands
J.Xiao-2@tudelft.nl

Lu Wang
Electrical Sustainable Energy
Delft University of Technology
Delft, The Netherlands
L.Wang-11@tudelft.nl

Pavol Bauer
Electrical Sustainable Energy
Delft University of Technology
Delft, The Netherlands
P.Bauer@tudelft.nl

Zian Qin
Electrical Sustainable Energy
Delft University of Technology
Delft, The Netherlands
Z.Qin-2@tudelft.nl

***Abstract*—This paper concerns the control problem of the active caused by the mismatched impedance in resistive feeders-dominated microgrids. A distributed model predictive control (DMPC) scheme is suggested to regulate the virtual impedance of each involved unit. Moreover, the proposed method benefits resilience to communication failure by designing the communication matrix. Furthermore, it involves propagating information among units in a short period, significantly reducing the communication and computation burden. Finally, the performance of the proposed control scheme is evaluated in terms of its convergence, robustness to communication delay and load variations, resilience to communication failure, and plug-and-play functionality without communication in an inverter-connected system.**

***Index Terms*—Model predictive control, adaptive virtual impedance, power sharing, distributed control.**

NOMENCLATURE

DG	Distributed generator
MG	Microgrids
ω_i	Output frequency of droop controller
ω_0	Nominal angular frequency
n_{qi}	Droop coefficient of reactive power loop
m_{pi}	Droop coefficient of active power loop
Q_i	Measured reactive power
P_i	Measured active power
V_i	Output voltage amplitude of droop controller
V_0	Nominal voltage amplitude
$V_{d,i}$	Output of droop controller
$V_{c,i}$	Filter capacitor voltage
$V_{r,i}$	Reference of filter capacitor voltage
V_{bus}	AC bus voltage
ΔV_i	Voltage drop across the feeder
i_o	Measured output current
Z_{load}	Load power
G_v	Gain of the voltage controller
Z_o	Output impedance of the inverter
Z_v	Virtual impedance
$Z_{L,i}$	Feeder impedance
$X_{l,i}$	Inductive components of the feeder
R_i	Resistive components of the feeder
x	State measurement of the microgrid
$\bar{x}$	Estimated average value of the microgrid
I_N	Identity matrix
G_{obs}	Observer transfer function
a_{ij}	Adjacency term
a_{ij}^e	Improved adjacency term
A	Adjacency matrix
A^e	Improved adjacency matrix
t_a	Neighbor's data delay
t_l	Local measurement delay
Γ	Trigger signal for deactivating communication
Θ	Steady state coefficient

I. INTRODUCTION

In microgrids (MGs), when with resistive line impedance, conventional droop control in [1], [2] can not achieve proportional active power sharing [3]. With the development of communication technology, [4], the cooperative control methodology of multi-agent systems has spurred the adoption of distributed secondary control as a reliable option as the distributed averaging proportional-integral (DAPI) scheme suggested in [5], [6]. This approach uses the proportional-integral-based secondary control to adjust the voltage and frequency compensation terms. However, this typical method predominantly employs PI controllers, which do not guarantee optimal solutions. Additionally, It fails to account for practical constraints in real-world applications [7]. When imposed uncertainty, these methods may yield irregular outputs.

To that end, the model predictive control (MPC) algorithm emerges as a viable solution, addressing the challenges associated with DAPI-based control by utilizing the predictive models to anticipate future system behavior [8]. It benefits physical limitation under uncertainty and optimal secondary layer output.

The distributed model predictive control (DMPC) has been reported to compensate the voltage for power sharing [8]–[11]. Each inverter autonomously addresses the local voltage optimization problem through a fully distributed approach, utilizing its forecasted actions and information from adjacent units. Notably, the introduction of DMPC algorithms raises two main concerns. First, their continuous prediction mechanisms may impose computational burdens that may be untenable in practical scenarios, especially when computational resources are limited [12]. Second, the distributed philosophy of DMPC emphasizes information propagation

979-8-3503-5133-0/24/$31.00 ©2024 IEEE

within the communication network, which may face challenges such as limited bandwidth, time delays, and traffic congestion. These communication constraints can significantly compromise the system's responsiveness [13]. The primary concern with DMPC arises from traditional methods' continuous communication and computation requirements. In these approaches, controllers operate in a time-triggered manner [10], performing data acquisition and control operations periodically [14]. As a result, this can lead to inefficient use of computational and communication resources since much of the data exchange and computation may not be necessary to achieve the desired overall system response.

To alleviate the communication and computational burden, event-triggered control using non-periodic communication is used in DMPC-based secondary control [15]. With the event-triggered mechanism [16], secondary control is activated only when the preset condition is triggered, achieving a relatively better control performance with limited communication resources. Furthermore, virtual impedance (VI) [17], [18] is another method for power compensation. Compared to the voltage compensation (VC) method in secondary control in [12], it features less communication dependency since extra computation is no longer needed once the virtual impedance is appropriately adjusted [3].

However, existing virtual impedance controls are based on DAPI [3], [19], limiting their ability to offer optimal adjustments and account for physical constraints in the secondary layer, as stated. To the best of the authors' knowledge, the distributed model predictive control-based virtual impedance control of the secondary layer has not been addressed in the existing research.

To address the limitations of conventional DAPI-based control, which does not account for physical constraints, and the challenges faced by existing DMPC-based methods, particularly those related to communication issues, this paper introduces a novel DMPC-based virtual impedance for secondary control in AC microgrids with resistive feeders. This algorithm optimizes the fundamental virtual impedance to improve active power sharing. In addition, further improvement of the control effectively mitigates problems arising from significant communication and computational burdens and communication failures.

II. Microgrid control and problem statement

A. Primary Control

To implement the power distribution among multiple parallel inverters with resistive feeders, the traditional control employs the droop law, whose P-V and Q-ω properties can be described as (1):

$$\omega_i = \omega_0 + n_{qi}Q_i; V_i = V_0 - m_{pi}P_i. \tag{1}$$

The internal controller usually consists of a voltage regulator and a current regulator, where the reference is the output of the droop control $V_{d,i}$. The inner loop controller's control block diagram can be represented as a voltage source in series with an impedance equivalent to $V_{r,i} = V_{d,i}{\cdot}G_v(s) - Z_o(s){\cdot}i_o$.

B. Active Power Analysis

The voltage drop across the feeder is affected by both resistance and inductance0 It is illustrated as presented in [17].

$$\Delta V_i = V_{c,i} - V_{bus} \approx \frac{X_{l,i}Q_i + R_iP_i}{V_{c,i}} \tag{2}$$

As the inductive component can be neglected in a resistive feeder MGs. (2) can be rewritten as (3):

$$\Delta V_i = V_{c,i} - V_{bus} \approx \frac{R_iP_i}{V_{c,i}} \tag{3}$$

Following (3), two methods exist for modifying the active power: changing the voltage reference $V_{r,i}$ and tuning the impedance of the feeder. In this research, we have employed the virtual impedance method due to its less reliance on a communication link. In this case, the reference voltage for the inner voltage controller is $V_r = V_d - Z_v i_o$.

III. The distributed model predictive control scheme

The proposed structure is illustrated in Fig.1, structured into four distinct parts: The primary control layer adopts the droop control. The distributed model predictive control is composed of a state observer for power regulation, predictive control, and cost function, and it is used to predict the system behavior and feed the reference to the virtual impedance layer. The integrator is used to eliminate the active power-sharing error. The propagated state variables active power $m_{pj}\bar{P}_j$ required for secondary control are exchanged on the communication layer. Additionally, to reduce communication costs, the information exchange among agents is governed by an embedded communication exit policy triggered by a predefined trigger condition Γ.

A. Communication Network Configure

the associated graph is modeled as undirected. The bidirectional connectivity from two nodes is defined by the adjacency term a_{ij}. It is defined that $a_{ij} = 1$ if the ith unit and the jth unit are in regular communication; otherwise, $a_{ij} = 0$. The communication adjacency matrix A=$(a_{ij})_{n\times n}$.

B. Power Transfer Equations

The relationship between active power and virtual fundamental impedance can be written as (4)-(5), where $B_i = 1/R_i$.

$$P_i(t) = B_i[V_{c,i}(t)^2 - V_{c,i}(t)V_{bus}^f(t)] \tag{4}$$

$$V_{c,i}(t) = V_{d,i} - i_{o,i}Z_{o,i} - i_{o,i}Z_{v,i}; V_{d,i}(t) = V_0 - m_{pi}P_i \tag{5}$$

C. Discrete Time Models

We derive a discrete model from equations (6)-(8) using the forward Euler method. Given integrators are linked at the output port of the predictive controllers to ensure zero steady-state error. We apply the incremental operator ($\Delta x(k) = [x(k) - x(k-1)]$) as described in the equations. Consequently, the optimization problem is formulated as a function of the variations in control actions ($Z_{v,i}$).

$$P_i(k+1) = P_i(k) + [V_{c,i}(k+1) - V_{c,i}(k)]B_i\Lambda_i \tag{6}$$

where $\Lambda_i = 2V_{c,i}(k) - V_{bus}(k)$. The dynamic state of bus voltage V_{bus} is ignored. Thus, an approximate first-order dynamic model of (4) can be discrete as (6). The discrete model of (5) corresponds to (7) and (8), respectively.

$$V_{c,i}(k+1) = V_{c,i}(k) + \Delta V_{d,i}(k+1) - i_{o,i}(k)\Delta Z_{v,i} \quad (7)$$

$$V_{d,i}(k+1) = V_{d,i}(k) - m_{pi}[P_i(k+1) - P_i(k)] \quad (8)$$

Notably, there are prediction errors in these models. For instance, both the dynamic models presented in (6) neglect to consider the dynamics of the bus voltage $V_{bus}(k)$, both of which are influenced by the interconnections among distributed generators. Nonetheless, these prediction errors do not exert a substantial impact on overall system performance when employing the proposed DMPC. This can be elucidated since the prediction errors at the current time step do not accumulate to affect subsequent time steps in MPC, where only the first step data is used for every calculated cycle. Furthermore, the output of the predictive algorithm provides the derivative of the calculated virtual impedance. In essence, the prediction errors only influence the virtual impedance change rate during dynamic processes. With the integrator, these errors are gradually eliminated as the system approaches a steady state, ultimately achieving accurate power sharing.

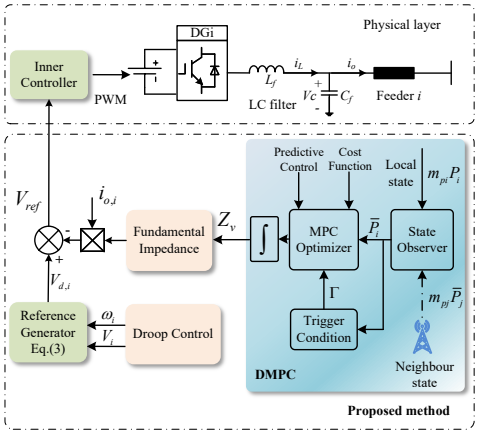

Fig. 1: The control diagram of the proposed method.

D. State Observer

The expressions of the dynamic average estimation for active power, which are the reference for the DMPC controller, are given in equations (9), respectively, where $\delta_i^p = m_{pi}P_i$. They are computed exclusively based on local measurements and information communicated from other generators. The adjacency term a_{ij} regulates communication.

$$\bar{\delta}_i^p(t) = \delta_i^p(t) + \int_0^t \sum_{j\in N_i} a_{ij}[\bar{\delta}_j^p(\tau) - \bar{\delta}_i^p(\tau)] \quad (9)$$

The operational constraints encompass a set of inequalities designed to guarantee that the performance of the distributed generators remains within physically feasible limits. In practice, these constraints ensure the virtual impedance is maintained within an appropriate range. The range can be derived by the secure voltage band [20], as the virtual impedance essentially affects the filter capacitor voltage. When the virtual impedance exceeds the threshold, it can adversely affect the bus voltage. Conversely, if the virtual impedance is too low, it may render the system unstable. This particular set of constraints is articulated in $Z_{v,i,min}(k) \le Z_{v,i} \le Z_{v,i,max}(k)$.

E. Cost Function

The output of DMPC is determined by a multi-objective cost function (10), which is constructed from two terms, each representing a control objective in the microgrid. Here, (11) describes the average active power-sharing control. While the optimization problem is local for every DG, the control is global for the whole microgrid since they are based on predictions transmitted by communicating. The second term (12) is used to minimize the control operations that are needed to match the goals. η_i represents the weighting coefficient.

$$\min_{ui} J_i(k) = J_i^P(k) + J_i^{zf}(k) \quad (10)$$

$$J_i^P(k) = \eta_i^p \sum\nolimits_{j=1}^{N} a_{ij}(k)[\delta_j^p(k+1) - \delta_i^p(k+1)]^2 \quad (11)$$

$$J_i^{zf}(k) = \eta_i^{zf}[\Delta Z_{v,i}]^2 \quad (12)$$

F. Relief to Communication Issues

1) Converge analysis: It's worth noting that (9), which establishes the averages for active power, incorporates the parameter a_{ij}, which indicates necessary communication between the relevant inverters. Besides, the adoption of DMPC imposes computation requirements. Herein, the average estimation can be simplified as (13). The local unit i estimates the average value of the system x_i by the local state and the neighbor's state $\bar{x}_j$. Then, $\bar{x}_i$ is fed to the MPC optimizer as the reference.

$$\bar{x}_i(t) = x_i(t) + \int_0^t \sum_{j\in N_i} a_{ij}[\bar{x}_j(\tau) - \bar{x}_i(\tau)] \quad (13)$$

The global dynamics can be written as $\dot{\bar{X}} = \dot{X} - L\bar{X}$. Where $X = [x_1, x_2 \cdots, x_N]^T$ denotes the measurements of the local units. $\bar{X}$ represents the estimated global average state. It is reported that with an undirected graph, all the participated inverters will converge to the average value of the system [21].

2) Communication delay analysis: Based on the dynamic average estimation in (13), when considering the communication delay, it can be expressed as (14).

$$\dot{\bar{x}}_i(t) = \dot{x}_i(t) + \sum_{j\in N_i} a_{ij}[\bar{x}_j(t-t_a) - \bar{x}_i(t-t_l)] \quad (14)$$

It is stated that this dynamic averaging algorithm achieves global consensus even under communication delay. This proof is omitted for brevity, as it was done in [22].

3) Communication failure analysis: In case of communication failure in the processing of the neighbor's information transfer, the data propagated through this communication link becomes null, which deteriorates the power-sharing performance. However, it is expected that under normal operating conditions, active power should not assume zero values, contributing to distinguishing communication failure.

Based on the a_{ij} definition, the constant zero is an ineffective state and is assigned a zero communication term. Consequently, the improved adjacent matrix a^e_{ij} ensures that only effectively received information is utilized to estimate and predict these averages.

4) Communication relief strategy: To reduce the communication and computational burden, we propose a trigger condition for identifying the deactivation of the communication network and MPC computation. In (15), Γ is introduced to indicate that the prediction algorithm and the state observer can be deactivated, which can be realized by forcing all elements of the adjacency matrix A to be zero. Γ=1 implies that the system has reached a state of proper adaptation, rendering the neighbor state unnecessary. Consequently, there is no need to propagate information for computation. This, in turn, leads to a state where the virtual impedance becomes completely self-sufficient, independent of the communication network and the MPC calculation.

$$\Gamma = \begin{cases} 1, & if \quad \Theta_1 \cap \Theta_2 \cdots \cap \Theta_N = 1 \\ 0, & else \end{cases} \tag{15}$$

where Θ assumes a binary value, representing the if the virtual impedance is appropriately set. Referring to (9), if the average power approximates the measured power, it signifies that power sharing is indeed proportionate, where the communication network and MPC can be disabled. To mitigate the potential influence of measurement noise, which can lead to minor power fluctuations, we introduce the condition that $\Theta_i = 1$, if the expression $[\bar{x}_i(k) - x_i(k)]/x_i(k) \leq 1\%$ hold true. Or else, Θ_i is set to 0.

IV. Simulation Evaluation

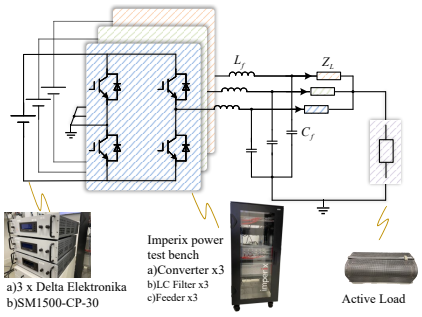

Fig. 2: Verification setup.

To demonstrate the superiority of the proposed method over existing methods, a three-inverter connected system is developed as depicted in Fig.2. In the setup, the output port of the converter is linked to the AC bus through a resistive feeder impedance (Z_L=0.5Ω) and an LC filter (C_f=12μF, L_f=2.2mH). The output active power ratios adhere to the maximum capacity proportion set at 1:2:3.

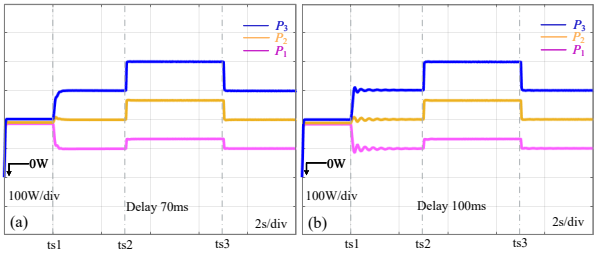

Fig. 3: Active power sharing performance comparison with the proposed method under communication delay:(a) DMPC with 70ms delay. (b) DMPC with 100ms delay.

Fig.3 provides a comprehensive investigation of the performance of active power sharing with different communication delays using the proposed method. Secondary control is enabled at *ts1*, and a 200W active load is increased and restored at *ts2* and *ts3*, respectively. It is claimed that the communication technologies used in microgrids have a latency of less than 100 ms [23], so in this paper, we test the power-sharing performance under 70ms and 100ms as shown in Fig.3(a) and (b), respectively. It can be seen that when suffering a 70ms delay, the active power exhibits good performance. When the inverter system is challenged by a 100ms delay, a slight oscillation is imposed but later attenuated. Therefore, this test shows that the proposed DMPC can maintain power sharing even under communication delay.

Fig.4(a) and (b) depict the significance of the physical constraints. Notably, when communication link 2-1 experiences an interruption at *ts4*, the controller based on the DAPI in [19] is afflicted by continuous adverse effects, shown in Fig.4(a). Conversely, the proposed DMPC-based secondary control successfully confines the perturbations in power references to a permissible range.

Moving on to Fig.4(c), (d) and (e), they describe the plug-and-play capacity of the methods in [10], [24], and the proposed DMPC, respectively, in scenarios where the communication network is disabled at *ts5*. These three approaches exhibit efficacy when communication is available. However, when the communication infrastructure is deactivated, the DMPC method expounded in [10], as shown in Fig.4(c), manifests ineffectiveness immediately, as well as the plug-and-play capacity. For the DMPC delineated in [24], as shown in Fig.4(d), the power-sharing during non-periodic communication can be guaranteed. However, the operational units' power-sharing ratio is not 1:2 during the stage between *ts6* and *ts7* where the $DG3$ is plugged out and re-plugged in, respectively. This observation indicates the dependency of existing methods on continuous communication and regular real-time calculations. Notably, the proposed method derives advantages from the conservation of communication and computational resources, shown in Fig.4(e).

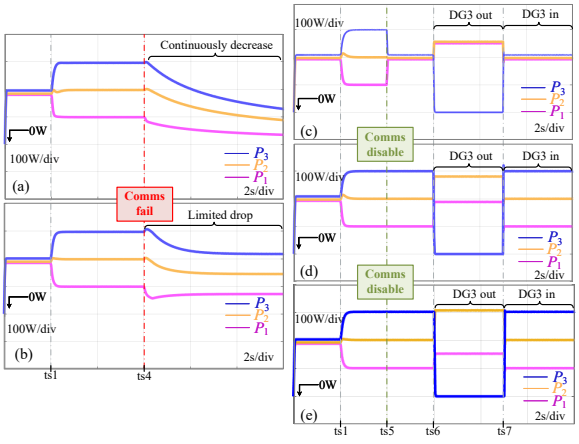

Fig. 4: Active power performance comparison:(a) DAPI in [19] without constraints. (b) the proposed DMPC. (c) plug-and-Play test of DMPC in [10]. (d) plug-and-Play test of DMPC in [24]. (e) plug-and-play test of the proposed DMPC.

V. Experiment Results

The experiments, investigating three critical scenarios, are conducted to demonstrate the sharpness and efficacy of the proposed DMPC method introduced in this paper. Notably, the experiment setup and control parameters are shown in Fig.2.

A. Performance in Power Sharing under Load Variations

The responses of the output active power of the involved inverters (P_1, P_2, P_3) are displayed in Fig.5. As can be seen from Fig.5, at the start of the experiment procedure (*t1-t2*), the output active power of all DGs will exhibit almost the same because of the feeder impedance and the output impedance's joint influence. However, the expected sharing ratio of $DG1$:$DG2$:$DG3$ is 1:2:3, according to the maximum output capacity of the inverter of the experiment setup. At *t2*, the proposed DMPC-virtual impedance-based secondary control is activated, contributing to the active power-sharing ratio shifts from 1:1:1 to 1:2:3.,which proved the effectiveness of the proposed method. The load changes at *t3*, where the output active power increases by 300W. In the *t3-t4* stage, the active power can still maintain 1:2:3; when it recovers to 600W at *t4*, the output active power of the inverters is changed to 100W, 200W, and 300W, respectively.

B. Resilience Investigation to Communication Failures

Further, the control performance of the proposed DMPC approach in the situation of communication failure is evaluated on the experimental platform. Fig.6 shows the performance of active power. The communication link 3-2 suffers a failure denoted in Fig.6.

To be specific, in *t6-t7*, the propagated information is in regular communication, and the power-sharing ratio is 1:2:3. In *t7-t8*, the transmitted data is forced to be zero due to the communication failure, which may distort the reference of the DMPC since the local DMPC controller computes the reference based on the received information. As it can be seen, in the *t6-t7* stage, the active power is no longer 1:2:3. Fortunately, the DMPC considers the physical constraints of the system, which means the virtual impedance can only be adjusted in an allowable range. This constraint can promise that the system will not oscillate and be unstable. At *t8*, the proposed resilient framework is activated, and the adjacent matrix A is replaced by A^e, thus disregarding the corrupted communication link. In other words, with the modification adjacent term $a^e_{i,j}(k)$, the corrupted propagated information will not be considered for power reference compute for the DMPC controller; Thus, it will not affect the output power. With the resilience method, the active power-sharing ratio returns to 1:2:3. The results demonstrate the resilience of the proposed method against communication failure.

C. Plug-and-Play Operation in AC Microgrids without Communication Dependencies:

To investigate the communication independence of the proposed DMPC approach regarding plug-and-play capability, we conduct the experimental scenarios as follows on the test platform established, where Fig.7 shows the active power performance, respectively.

First, the communication network is deactivated at *t10*. It can be seen that active power sharing performance can remain 1:2:3. Subsequently, $DG3$ is assumed to be inaccessible and plugged out at *t11* and then be back and connected to the MG at *t=t12*. In contrast, $DG2$ is plugged out at *t12* and reconnected at *t14*.

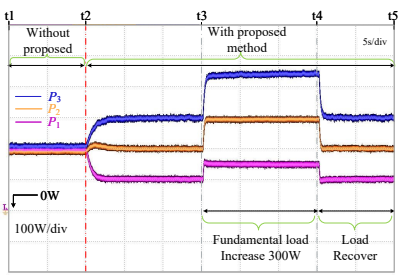

Fig. 5: Active power sharing performance of the designed controller.

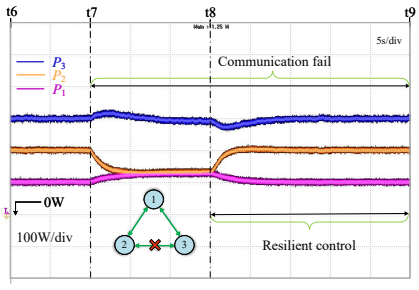

Fig. 6: The resilience of the proposed method against communication failure.

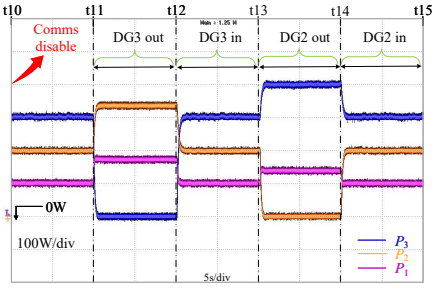

Fig. 7: Communication independence verification.

During *t11-t12*, as $DG3$ is de-plugged, its physical link connected to the inverter-connected system is lost. The tie lines from $DG3$ to $DG1$ and from $DG3$ to $DG2$ are considered open circuits. Meanwhile, the coordinated distributed predictive control scheme is inactive for $DG3$ during *t11-t12*. The proposed DMPC also does not need to be effective for the active power regulation of the remaining DGs in the microgrid since the virtual impedance has been appropriately set. In this period, the output active of $DG3$ is 0W. Thanks to the pre-adjusted virtual impedance, the operational units $DG1$ and $DG2$ maintain a power-sharing ratio of 1:2, following the expected ratio. Similarly, during *t13-t14*, the $DG2$ is plugged out, thus outputting 0W active power. The operational $DG1$ and $DG3$ exhibit a power-sharing ratio of 1:3. During *t12-t13* and *t14-t15*, the plugged-out unit is replugged in the microgrid, and the power-sharing proportion is recovered to 1:2:3 among the three inverters. The DMPC-based secondary control benefits plug-and-play capacity even if there is no communication since the virtual impedance has been pre-adjusted and fixed, thus independent of the communication network.

VI. Conclusion

This paper introduces a distributed model predictive control-based virtual impedance method to manage active power in resistive feeder microgrids. With this approach, each unit within the microgrid adjusts its virtual impedance parameters based on exchanged information. Notably, the proposed DMPC scheme exhibits a robust capability for load switches under communication delays. Furthermore, a well-designed communication matrix demonstrates resilience in communication failures. The method suggested alleviates the computational and communication burdens compared to prior literature. Through information exchange over a brief duration, this approach ensures the desired power-sharing performance and supports plug-and-play operation, even when the communication network becomes inaccessible at a later stage. The proposed method's effectiveness and its comparative analysis with existing techniques are validated through experimental and simulation results.

References

[1] J. Xiao, Y. Jia, B. Jia, Z. Li, Y. Pan, and Y. Wang, "An inertial droop control based on comparisons between virtual synchronous generator and droop control in inverter-based distributed generators," *Energy Reports*, vol. 6, pp. 104–112, 2020.

[2] Y. Jia, J. Xiao, B. Jia, Y. Pan, Y. Wang, and Z. Li, "Improved droop control based on multi-stage lead-lag compensation," in *IECON 2020 The 46th Annual Conference of the IEEE Industrial Electronics Society*. IEEE, 2020, pp. 3224–3229.

[3] J. Xiao, L. Wang, P. Bauer, and Z. Qin, "Virtual impedance control for load sharing and bus voltage quality improvement in low voltage ac microgrid," *IEEE Transactions on Smart Grid*, pp. 1–1, 2023.

[4] J. Xiao, L. Wang, Z. Qin, and P. Bauer, "Detection of cyber attack in smart grid: A comparative study," in *2022 IEEE 20th International Power Electronics and Motion Control Conference (PEMC)*. IEEE, 2022, pp. 48–54.

[5] ——, "An adaptive cyber security scheme for ac micro-grids," in *2022 IEEE Energy Conversion Congress and Exposition (ECCE)*. IEEE, 2022, pp. 1–6.

[6] J. W. Simpson-Porco, Q. Shafiee, F. Dörfler, J. C. Vasquez, J. M. Guerrero, and F. Bullo, "Secondary frequency and voltage control of islanded microgrids via distributed averaging," *IEEE Transactions on Industrial Electronics*, vol. 62, no. 11, pp. 7025–7038, 2015.

[7] J. Xiao, L. Wang, Z. Qin, and P. Bauer, "A resilience enhanced secondary control for ac micro-grids," *IEEE Transactions on Smart Grid*, pp. 1–1, 2023.

[8] A. N. F., J. S. Gómez, J. Llanos, E. Rute, D. Sáez, and M. Sumner, "Distributed predictive control strategy for frequency restoration of microgrids considering optimal dispatch," *IEEE Transactions on Smart Grid*, vol. 12, no. 4, pp. 2748–2759, 2021.

[9] E. Rute-Luengo, A. Navas-Fonseca, J. S. Gómez, E. Espina, C. Burgos-Mellado, D. Sáez, M. Sumner, and D. Muñoz-Carpintero, "Distributed model-based predictive secondary control for hybrid ac/dc microgrids," *IEEE Journal of Emerging and Selected Topics in Power Electronics*, vol. 11, no. 1, pp. 627–642, 2023.

[10] Q. Yang, J. Zhou, X. Chen, and J. Wen, "Distributed mpc-based secondary control for energy storage systems in a dc microgrid," *IEEE Transactions on Power Systems*, vol. 36, no. 6, pp. 5633–5644, 2021.

[11] Y. Yu, G.-P. Liu, and W. Hu, "Coordinated distributed predictive control for voltage regulation of dc microgrids with communication delays and data loss," *IEEE Transactions on Smart Grid*, vol. 14, no. 3, pp. 1708–1722, 2023.

[12] A. Navas-Fonseca, C. Burgos-Mellado, J. S. Gómez, F. Donoso, L. Tarisciotti, D. Sáez, R. Cárdenas, and M. Sumner, "Distributed predictive secondary control for imbalance sharing in ac microgrids," *IEEE Transactions on Smart Grid*, vol. 13, no. 1, pp. 20–37, 2022.

[13] T. Zhao, Z. Li, and Z. Ding, "Consensus-based distributed optimal energy management with less communication in a microgrid," *IEEE Transactions on Industrial Informatics*, vol. 15, no. 6, pp. 3356–3367, 2019.

[14] T. Yang, S. Sun, and G.-P. Liu, "Distributed discrete-time secondary cooperative control for ac microgrids with communication delays," *IEEE Transactions on Industrial Electronics*, vol. 70, no. 6, pp. 5949–5959, 2023.

[15] P. Ge, B. Chen, and F. Teng, "Event-triggered distributed model predictive control for resilient voltage control of an islanded microgrid," *International Journal of Robust and Nonlinear Control*, vol. 31, no. 6, pp. 1979–2000, 2021.

[16] X. Chen, H. Yu, and F. Hao, "Prescribed-time event-triggered bipartite consensus of multiagent systems," *IEEE Transactions on Cybernetics*, vol. 52, no. 4, pp. 2589–2598, 2022.

[17] J. Xiao, L. Wang, Z. Qin, and P. Bauer, "Virtual impedance control for load sharing and bus voltage quality improvement," in *2023 25th European Conference on Power Electronics and Applications (EPE'23 ECCE Europe)*, 2023, pp. 1–8.

[18] ——, "An adaptive virtual impedance control for reactive power sharing in microgrids," in *2023 IEEE Energy Conversion Congress and Exposition (ECCE)*, 2023, pp. 584–589.

[19] Z. Wang, Y. Chen, X. Li, Y. Xu, W. Wu, S. Liao, H. Wang, and S. Cao, "Adaptive harmonic impedance reshaping control strategy based on a consensus algorithm for harmonic sharing and power quality improvement in microgrids with complex feeder networks," *IEEE Transactions on Smart Grid*, vol. 13, no. 1, pp. 47–57, 2022.

[20] D. G. Photovoltaics and E. Storage, "Ieee standard for interconnection and interoperability of distributed energy resources with associated electric power systems interfaces," *IEEE Std*, vol. 1547, pp. 1547–2018, 2018.

[21] V. Nasirian, S. Moayedi, A. Davoudi, and F. L. Lewis, "Distributed cooperative control of dc microgrids," *IEEE Transactions on Power Electronics*, vol. 30, no. 4, pp. 2288–2303, 2014.

[22] X. Chen, J. Zhou, M. Shi, Y. Chen, and J. Wen, "Distributed resilient control against denial of service attacks in dc microgrids with constant power load," *Renewable and Sustainable Energy Reviews*, vol. 153, p. 111792, 2022.

[23] C. Kalalas, L. Thrybom, and J. Alonso-Zarate, "Cellular communications for smart grid neighborhood area networks: A survey," *IEEE access*, vol. 4, pp. 1469–1493, 2016.

[24] A. Navas-Fonseca, C. Burgos-Mellado, J. S. Gómez, E. Espina, J. Llanos, D. Śaez, M. Sumner, and D. E. Olivares, "Distributed predictive secondary control with soft constraints for optimal dispatch in hybrid ac/dc microgrids," *IEEE Transactions on Smart Grid*, pp. 1–1, 2023.